STEM CELLS®

STEM CELL TECHNOLOGY: EPIGENETICS, GENOMICS, PROTEOMICS, AND METABONOMICS

Proliferation State and Polo-Like Kinase1 Dependence of Tumorigenic Colon Cancer Cells

FEDERICA FRANCESCANGELI,[a] MICHELE PATRIZII,[a] MICHELE SIGNORE,[a] GIULIA FEDERICI,[a] SIMONE DI FRANCO,[b] ALFREDO PAGLIUCA,[a] MARTA BAIOCCHI,[a] MAURO BIFFONI,[a] LUCIA RICCI VITIANI,[a] MATILDE TODARO,[b] RUGGERO DE MARIA,[c] ANN ZEUNER[a]

[a]Department of Hematology, Oncology and Molecular Medicine, Istituto Superiore di Sanità, Rome, Italy; [b]Department of Surgical and Oncological Sciences, University of Palermo, Palermo, Italy; [c]Istituto Nazionale Tumori Regina Elena, Rome, Italy

Key Words. Cancer stem cells • Colorectal cancer • Cell proliferation • Cell cycle

ABSTRACT

Tumor-initiating cells are responsible for tumor maintenance and relapse in solid and hematologic cancers. Although tumor-initiating cells were initially believed to be mainly quiescent, rapidly proliferating tumorigenic cells were found in breast cancer. In colon cancer, the proliferative activity of the tumorigenic population has not been defined, although it represents an essential parameter for the development of more effective therapeutic strategies. Here, we show that tumorigenic colon cancer cells can be found in a rapidly proliferating state in vitro and in vivo, both in human tumors and mouse xenografts. Inhibitors of polo-like kinase1 (Plk1), a mitotic kinase essential for cell proliferation, demonstrated maximal efficiency over other targeted compounds and chemotherapeutic agents in inducing death of colon cancer-initiating cells in vitro. In vivo, Plk1 inhibitors killed CD133$^+$ colon cancer cells leading to complete growth arrest of colon cancer stem cell-derived xenografts, whereas chemotherapeutic agents only slowed tumor progression. While chemotherapy treatment increased CD133$^+$ cell proliferation, treatment with Plk1 inhibitors eliminated all proliferating tumor-initiating cells. Quiescent CD133$^+$ cells that survived the treatment with Plk1 inhibitors could be killed by subsequent Plk1 inhibition when they exited from quiescence. Altogether, these results provide a new insight into the proliferative status of colon tumor-initiating cells both in basal conditions and in response to therapy and indicate Plk1 inhibitors as potentially useful in the treatment of colorectal cancer. STEM CELLS *2012;30:1819–1830*

Disclosure of potential conflicts of interest is found at the end of this article.

INTRODUCTION

Every year more than 1 million people worldwide develop colorectal cancer, with a mortality of approximately 33% in developed countries [1]. In the past 5 years, the use of targeted agents has brought an improvement of survival outcomes for selected categories of colorectal cancer patients. However, a large portion of patients will not benefit by treatment with monoclonal antibodies and relies on 5-fluoropyrimidine-based chemotherapeutic regimens. The discovery of cancer stem cells (CSC) in solid tumors drew a different perspective on antineoplastic therapies, following the demonstration that CSC are extremely resistant to cytotoxic stimuli in vitro and in vivo as a result of hyperactive DNA repair pathways, drug efflux mechanisms, or decreased production of reactive oxygen species [2–4]. Colon CSC were characterized on the basis of CD133, Lgr5, or aldehyde dehydrogenase 1 (ALDH 1) expression [5] and were subsequently shown to be particularly resistant to chemotherapeutic agents [6], possibly explaining the inability of chemotherapy to eradicate colorectal tumors. Therefore, it is of primary importance to identify pathways active in CSC that could represent the target for new antitumor therapies.

CSC proliferation status is highly relevant for cancer therapy. However, while the proliferative activity of stem cells in normal adult tissues and hematologic cancers has been thoroughly investigated, the proliferation of CSC from solid tumors has only recently started to be explored. Mammary CSC have been shown to possess an increased replicative

Author contributions: F.F.: performed data acquisition, analysis and interpretation, and contributed to study design; M.P.: performed animal experiments; M.S.: performed acquisition of data and statistical analysis; G.F. and S.D.F.: contributed to data acquisition; A.P.: genetically characterized colon cancer stem cell lines; M.B.: contributed to animal experiments; L.R.V. and M.T.: cancer stem cell line generation; M.B.: provided support for flow cytometry and data interpretation; R.D.M.: contributed to study design and provided critical revision of the manuscript; A.Z.: data acquisition and interpretation and study design and manuscript writing.

Correspondence: Ann Zeuner, Ph.D., Department of Hematology, Oncology and Molecular Medicine, Istituto Superiore di Sanità, 00161 Rome, Italy. Telephone: 39-06-49902479; Fax: 39-06-49387087; e-mail: a.zeuner@iss.it Received January 18, 2012; accepted for publication June 12, 2012; first published online in STEM CELLS *EXPRESS* June 29, 2012. 1066-5099/2012/$30.00/0 doi: 10.1002/stem.1163

potential as compared to their normal counterparts and to undergo more frequent self-renewing divisions [7]. In breast cancer, these properties are likely responsible for the continuous expansion of the CSC pool, while the ability of CSC to divide asymmetrically accounts for the production of more differentiated tumor cells. Normal colon stem cells have been shown to be actively cycling [8] and to stop dividing when they differentiate, but the proliferative status of their tumor counterpart has never been investigated in detail.

Polo-like kinase1 (Plk1) is a serine-threonine kinase that was originally identified in *Drosophila* as an essential mitotic regulator [9]. The expression of Plk1 is low in most adult tissues except for those with a high proliferative index. Conversely, a broad spectrum of human tumors overexpress Plk1, supporting the theory that an elevated expression of PLK1 is a general feature of human cancer [10]. Plk1 inhibition is considered a promising therapeutic approach in anticancer treatment, and a first wave of phase I studies aimed at identifying the maximum-tolerated dose has been recently completed. The Plk1 inhibitor volasertib (BI 6727) has moved to phase II in order to determine its antitumor activity and safety profile. Preliminary results from a clinical trial with volasertib as single-agent showed encouraging antitumor activity, with nonhematologic adverse events that were mild and uncommon [11]. We show that colon cancer-initiating cells (CCIC) are actively proliferating both in vitro and in vivo, overexpress Plk1, and are sensitive to Plk1 inhibitors. Importantly, Plk1 inhibitors showed enhanced antitumor activity on CCIC-derived xenografts as compared to chemotherapy, pointing to Plk1 as a potential therapeutic target in colorectal cancer.

Materials and Methods

Cells

Colon cancer specimens were obtained from patients undergoing surgical resection upon informed consent and approval by the Institutional Ethical Committee, and subsequent studies were conducted according to the Helsinki Declaration guidelines. CCIC were selected as previously described (6) and cultured as multicellular spheroids composed of $CD133^+$ cells in serum-free medium containing epidermal growth factor 20 ng/ml and basic fibroblast growth factor 10 ng/ml (PeproTech, London, U.K., http://www.peprotech.com). CCIC differentiation was obtained by culture in keratinocyte serum-free medium (KSFM) medium or in 10% serum-containing Dulbecco's modified Eagle's medium (both from Gibco-Invitrogen, Carlsbad, CA, http://www.invitrogen.com) for 10 days and confirmed by a decrease in CD133 and Lgr5 expression. Freshly isolated colon cancer cells were isolated from human tumor specimens or from CCIC-derived xenografts by magnetic cell separation with CD133/1 antibody-conjugated microbeads (Miltenyi Biotec, Bergisch Gladbach, Germany, http://www.miltenyibiotec.com). To obtain the human CD133− fraction, xenograft-derived CD133− cells were additionally sorted with an anti-human epithelial cell adhesion molecule (EpCAM) antibody.

Antibodies and Reagents

BI 2536 was purchased from Axon Medchem (Groningen, The Netherlands, http://www.axonmedchem.com). Terminal deoxynucleotidyl transferase dUTP nick end labeling (TUNEL) was from Roche Molecular Biochemicals (Indianapolis, IN, http://www.roche.com). CD133/1-phycoerythrin (PE) (used for flow cytometry/sorting) and CD133/2 (used for immunofluorescence) were from Miltenyi Biotec. Alexa Fluor-conjugated secondary antibodies were from Invitrogen-Molecular Probes (Eugene, OR, http://www.invitrogen. com). Anti-PLK1, Ki67, p-ATM, and anti-cyclin B1 antibodies were from Santa Cruz (Santa Cruz, CA, http://www.scbt.com). Caspase 3 and 9 antibodies were from Millipore-Upstate Biotechnology (Billerica, MA, http://www.millipore.com). Monoclonal anti-α-tubulin was from Sigma Aldrich (St Louis, MO, http://www.sigmaaldrich.com). Aurora aurora/IPL1-related kinase (A/AIK) and anti-phospho-histone H3 (Ser10) were from Cell Signaling Technology (Beverly, MA, http://www.cellsignal.com). Secondary anti-mouse and anti-rabbit antibodies coupled to horseradish peroxidase (HRP) were from GE Healthcare (Uppsala, Sweden, http://www.gehealthcare.com). M30 antibody was from Peviva AB (Bromma, Sweden, http://www.peviva.com), and Lgr5 antibody was from Abgent (San Diego, CA, http://www.abgent.com).> The ALDEFLUOR assay was from Aldagen, (Durham, NC, http://www.aldagen.com). The APC bromodeoxyuridine (BrDU) Flow Kit was from BD Biosciences (San Diego, CA, http://www.bdbiosciences.com).

PKH Staining

CCIC spheroids were dissociated with TrypLE Express (Invitrogen) and stained for 2 minutes at 37°C with 1:500 PKH-26 dye (Sigma-Aldrich, St. Louis, http://www.sigmaaldrich.com), then washed extensively with PBS, and cultured for 10 days. Cells were then sorted with a fluorescence-activated cell sorting (FACS) Aria (Becton Dickinson, Franklin Lakes, NJ, http://www.bd.com) into PKH-low/negative, -intermediate, and -high fractions. Control cells did not undergo PKH-26 staining but were mock-sorted to induce similar stress conditions as in the other sorted samples.

Plk1 RNA Interference

A total of 1.25×10^5 CCSC were plated on six-well plates in antibiotic-free culture medium and incubated for 4 hours at 37°C in the presence of 320 nM ON-TARGETplus SMARTpool short-interfering RNA (siRNA) (J-003290-00-0005, Human PLK1, NM_005030) or control siRNA (nontargeting siRNA D-001810-01) (Thermo Scientific, Lafayette CO, http://www.thermoscientific.com) and 5 μl Lipofectamine 2000 (Invitrogen). After 4 hours, the transfection mixture was substituted with normal growth medium, and cells were analyzed for Plk1 expression, viability, and morphology at the indicated times.

Library Screening

CCIC spheroids were dissociated with TrypLE Express and 3,000 cells per well were seeded in 96-well microtiter plated at day 0. On day 2, cells were treated with a library of kinase inhibitors (Enzo Life Sciences, New York, NY, http://www.enzolifesciences.com) used at a 100 nM concentration. In addition, the following compounds were used at a concentration of 100 nM: BI 2536, Met kinase inhibitor (PHA-665752), and Aurora kinase inhibitor (PHA-680632) (both from Selleck Chemicals, Houston, TX, http://www.selleckchem.com). 5-Fluorouracil (5-FU) and Oxaliplatin (OXA) (Sigma-Aldrich) were added at a final concentration of 10 μM, which approximates peak plasma values in treated patients. Cells were processed after 48 hours with the CellTiter-Glo viability assay (Promega, Madison, WI, http://www.promega.com) according to manufacturer's instructions, and the luminescent signal was read on a DTX880 microplate reader (Beckman Coulter, Brea, CA, http://www.beckmancoulter.com). Viability was calculated as follows: Vs/Mc × 100, where Vs represents the integrated intensity of luminescence counts from the treated sample and Mc represents the average of the integrated intensities of luminescence counts from the dimethyl sulfoxide (DMSO) control.

Cell cycle, Apoptosis, and Clonogenicity Assays

The cell cycle status of CCSC was assessed by staining dissociated spheroids with 50 μg/ml propidium iodide dissolved in buffer 0.1% trisodium citrate, 9.65 mM NaCl, 0.1% Nonidet P40, and 200 μg/ml RNase for 1 hour at room temperature. Samples were analyzed with a FACSCanto flow cytometer (Becton Dickinson) equipped with a DIVA software. The CellTiter-Glo assay (Promega) was used to determine cell viability. A total of 2×10^3 dissociated cells were plated at day 0 in 96-well flat bottom plates. 100 nM BI 2536, 200 mg/ml His-Flag TRAIL, or 40 μM

zVAD (Bachem, Bubendorf, Switzerland) were added at day 1, and cells were processed at day 3 according to the manufacturer's instructions. Luminescent signal was read using DTX880. Clonogenicity assay of CCSC was performed by plating 500 single cells per well in triplicate suspended in 0.3% agarose with or without BI 2536 over a layer of 0.4% agarose. Plates were incubated in a 5% CO_2 humidified incubator at 37°C, and colony counts were performed 20–25 days after plating. The colonies were stained with crystal violet (0.1% in 10% MetOH) and counted under a light microscope. Data shown represent the percentage of colony numbers relative to plated cells.

Mice Treatment

Animal experiments were conducted according to the national Animal Experimentation guidelines (D.L.116/92) upon approval of the experimental protocol by the Institutional Animal Experimentation Committee. 6–8-week-old female non-obese diabetic (NOD). Cg-Prkdc^{scid} Il2rg^{tm1Wjl}/SzJ (NSG) mice (The Jackson Laboratory, Bar Harbor, ME, http://www.jax.org) were subcutaneously injected with the following number of cells resuspended in 100 μl Matrigel/CCIC medium 1:1. For BI 6727 or chemotherapy treatment, we used 2.5 $\times$ 10^5 cells; for the PKH experiment of Figure 1, we used 2.5 $\times$ 10^3 cells; for PKH limiting dilution experiments, we used cell numbers indicated in Supporting Information Table 1. Pharmacological treatments with BI 6727 or chemotherapeutic agents were started when tumor xenografts reached an approximate volume of 100 mm^3. The BI 6727 group ($n = 6$) was treated by injecting endovenously the compound for 2 consecutive days each week (60 mg/kg weekly) dissolved in 1 N HCl 0.9% NaCl. The chemotherapy group ($n = 6$) was treated by injecting intraperitoneally the compounds (OXA 10 mg/kg, 5-FU 25 mg/kg) resuspended in phosphate buffer saline (PBS) once a week. The vehicle group ($n = 6$) was treated by injecting endovenously 100 μl 1 N HCl 0.9% NaCl twice a week. Tumor volume was evaluated by using an external digital caliper, and mice weight was evaluated at the indicated times. Mice were sacrificed 3 weeks after the beginning of the treatment, and tumors were removed, weighted, and either embedded in optimal cutting temperature compound (OCT) and frozen at −80°C or processed for subsequent flow cytometry/sorting. For short-term treatments, the BI 6727 group ($n = 6$) was injected endovenously with the compound (40 mg/kg) dissolved as described above, while the vehicle group ($n = 6$) was injected with 1 N HCl 0.9% NaCl. After 24 or 48 hours, mice were sacrificed and tumors were removed, embedded in OCT, and frozen at −80°C.

Immunofluorescence

CCIC spheroids were cytospun at low speed on polylysine-coated glass slides, whereas differentiated colon cancer cells were grown on Matrigel-coated coverslips. Typically, cells were fixed in 4% paraformaldehyde and permeabilized in 0.1% Triton X-100 (Bio-Rad Laboratories, Richmond, CA, http://www.bio-rad.com) then incubated overnight at 4°C with primary antibodies dissolved in PBS containing 3% bovine serum albumin (BSA), 0.1% Triton X-100. After two washes in PBS, cells were incubated with Alexa Fluor-conjugated secondary antibodies for 30 minutes at room temperature in the dark, stained for 15 minutes with 4′,6-diamidino-2-phenylindole (DAPI) (Invitrogen), diluted in PBS 3% BSA, and mounted with Prolong-Gold antifade (Invitrogen). For actin staining, cells were incubated for 30 minutes at room temperature with Alexa Fluor 488 phalloidin 1 μM (Invitrogen). For mitochondrial staining, live cells were incubated for 30 minutes at 37°C with 100 nM Mitotracker CMXRos (Invitrogen) then processed for staining with cytochrome c antibody as described above. Slides were analyzed on a FV1000 confocal microscope (Olympus, Tokyo, Japan, http://www.olympus-global.com) equipped with ×60 and ×40 oil immersion objectives.

Flow Cytometry and Sorting

Mitochondrial membrane depolarization was measured by flow cytometry following incubation of dissociated cells with 10 μg/ml tetramethyl rhodamine methyl ester (Invitrogen Molecular Probes) for 30 minutes at 37°C. For isolation of cells from xenograft tissue, cells were labeled with EpCAM-fluorescein isothiocyanate (FITC) (Dako, Glostrup, Denmark, http://www.dako.com) and CD133/1 PE (Miltenyi Biotec) for 30 minutes at room temperature and sorted with a FACS Aria (Becton Dickinson). 10 μg/ml 7-aminoactinomycin D (Sigma-Aldrich) was always added for dead cell exclusion.

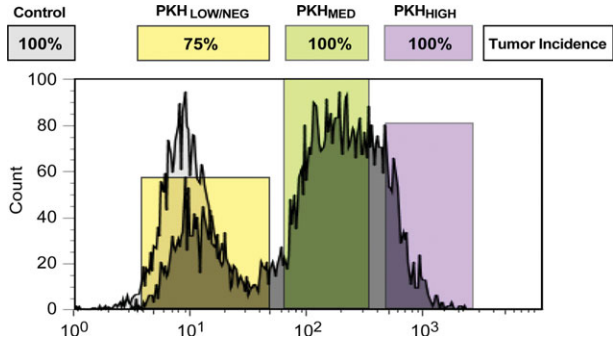

Figure 1. All the proliferative subsets of CD133$^+$ cells generate tumors in mice. CD133$^+$ cells derived from a colon tumor specimen were cultured as multicellular spheroids (DN08 colon cancer-initiating cell [CCIC] line), stained with the PKH-26 dye and, after 10 days, separated into three fractions according to PKH-26 retention. Sorted cells were inoculated subcutaneously into NOD.Cg-Prkdc^{scid} Il2rg^{tm1Wjl}/SzJ mice (eight per group). The percentage of tumors that arose from the different fractions (tumor incidence) is shown above.

Western Blotting

Cell lysates were obtained from approximately 2.5 $\times$ 10^5 colon cancer initiating cells (CCIC) by incubation of cell pellets in 1% Nonidet P40 lysis buffer (20 mM Tris-HCl pH 7.2, 200 mM NaCl, 1% Nonidet P40) supplemented with protease inhibitor cocktail and phosphatase inhibitor cocktails I and II (all from Sigma-Aldrich). Lysate concentrations were determined by the Bradford assay (Bio-Rad Laboratories, Hercules, CA), and equal amounts of proteins were loaded on a 4%–12% precast gel (Invitrogen) and transferred to nitrocellulose membranes. Blots were blocked with tris-buffered saline Tween-20 (TBST) 5% nonfat dry milk and incubated overnight at 4°C with primary antibodies, then incubated for 45 minutes with secondary HRP-conjugated antibodies dissolved in TBST 1% BSA. Chemiluminescent signals were detected with Super SignalWest Pico (Pierce, Rockford, IL, http://www.piercenet.com).

Immunohistochemistry

Tumor sections (5–8 μm) were obtained using a cryomicrotome (Kriostat 1720 MGW Leitz, Melville, NY, http://www.leitz.com). For CK18 staining, frozen sections were fixed in ice-cold methanol for 4 minutes, endogenous peroxidase activities were blocked using 0.03% hydrogen peroxide for 15 minutes in the dark, and then the sections were incubated at room temperature for 1 hour with M30 antibody. Sections were then processed using avidin-biotin-peroxidase complex (ULTRATEK HRP SCY, Tek Laboratories, West Logan, UT, http://teklabs.com), counterstained with hematoxylin, and mounted with DPX (Sigma-Aldrich). For immunofluorescence analysis, frozen sections were fixed in 4% paraformaldehyde, permeabilized in 0.1% Triton X-100, and blocked with 5% serum in PBS containing 1% BSA and 0.1% Triton X-100. Sections were stained overnight at 4°C with primary antibodies, incubated with fluorochrome-conjugated secondary antibodies with 5 mg/ml RNase A, and counterstained with DAPI. TUNEL staining was performed with the In Situ Cell Death Detection Kit (Roche Molecular Biochemicals) according to the manufacturer's instructions. Azan-Mallory staining was performed on xenograft cryosections with the Mallory Tricromica kit (Bio-Optica, Milan, Italy, http://www.bio-optica.it) according to the manufacturer's instructions.

Statistical Analysis

Unless otherwise specified, statistical analysis was conducted by using two-way ANOVA, and differences between groups/pairs were evaluated with Bonferroni post tests. Analysis of Figure 6E was performed with two-tailed unpaired *t* test. Statistical analysis was performed with GraphPad Prism v.4.0 for Windows (GraphPad Software, San Diego, CA, www.graphpad.com), and statistical significance was accepted up to .05. *p* values are displayed using a single asterisk for significances ranging from .05 to .01, two asterisks for values between .001 and .01, and three when statistical differences produced significance below .001.

RESULTS

Tumorigenic Colon Cancer Cells Are Present in All Proliferative Subsets of CD133$^+$ Cells

CD133$^+$ colon cancer cells have been previously shown to be enriched for cells with tumorigenic ability [12, 13]. To investigate the proliferative state of CCIC, we separated different subsets of CD133$^+$ CCIC according to their proliferative activity and then tested their ability to generate tumors in immunocompromised mice. To do so, CD133$^+$ cells derived from surgical specimens were cultured as multicellular spheroids and stained with the fluorescent dye PKH-26, which binds cell membranes and segregates in daughter cells after each cell division, thus providing a signal that correlates with the cell's proliferation history. After 10 days of PKH staining, CCIC were FACS-separated into three subsets, $PKH_{LOW/NEG}$ (very rapidly proliferating), PKH_{MED} (rapidly proliferating), and PKH_{HIGH} (slowly proliferating). Sorted cells were immediately inoculated in NSG mice (2.5×10^3 cells each), and subcutaneous tumor formation was observed after approximately 2 months. Cells belonging to the PKH_{MED} and PKH_{HIGH} fractions gave rise to tumors in 100% of mice, as did bulk control cells from unstained cultures (Fig. 1). Surprisingly, however, also cells of the $PKH_{LOW/NEG}$ subset gave rise to tumors, although with lower efficiency as compared with the two other subsets (Fig. 1). These results were substantiated by limiting dilution experiments showing, in three different CCIC samples, the presence of tumorigenic cells in variable amounts in the $PKH_{LOW/NEG}$ fraction (Supporting Information Table 1). Results from in vitro colony forming assays confirmed these observations, showing that all three PKH cell subsets were endowed with colony-forming efficiency (data not shown). PKH distribution was also investigated in cultured CCIC in relation to ALDH activity, which was previously indicated as a colon stem cell marker [14]. The starting cell population, composed of 100% CD133$^+$ cells, was separated in $PKH_{LOW/NEG}$, PKH_{MED}, and PKH_{HIGH} 10 days after PKH staining, and ALDH activity was measured in the three fractions with the ALDEFLUOR kit. ALDH$^+$ cells were comparably distributed among the different PKH fractions, again suggesting an equivalent content of tumorigenic cells (Supporting Information Fig. S1). These observations indicate that colon tumor-initiating cells are found both in slow and fast proliferative states, and they can undergo rapid cell division without losing their tumorigenic potential.

CCIC Express High Levels of Plk1 and Are Highly Sensitive to Plk1 Inhibition

Proliferating cells express high levels of the mitotic kinase Plk1. To determine whether high Plk1 levels were associated with the CCIC compartment, we investigated Plk1 expression in colon cancer cells freshly isolated from surgical specimens or from tumor xenografts. CD133$^+$ tumor cells isolated either from human tumors or from CCIC-derived mouse xenografts expressed higher levels of Plk1 as compared with CD133$^-$ cells (Fig. 2A), thus suggesting that a highly proliferating state may be typical of the colon CSC population in vivo. The correlation between "stemness" and Plk1 expression was confirmed by comparing seven patient-derived spheroid cultures (described in Supporting Information Table 2) with their differentiated progeny, composed of adherent cells that have lost CD133 and Lgr5 expression (Supporting Information Fig. S2). As expected, Plk1 was more expressed in the stem cell fraction (Fig. 2B) and was mainly localized on centrosomes of dividing cells (Supporting Information Fig. S3A). The higher Plk1 expression in CD133$^+$ CCIC observed in vitro and in vivo parallels the elevated proliferative activity of CD133$^+$ cells. In fact, we observed that in vitro CCIC proliferate more than their differentiated counterparts (Supporting Information Fig. S4A, S4B), and that in CCIC-derived tumor xenografts, CD133 expression was mainly associated with Ki67 staining (Supporting Information Fig. S4C). Due to the high expression of Plk1 in the CCIC compartment, we ought to investigate the effect of the Plk1 inhibitor BI 2536 on CCIC in comparison to a panel of 80 targeted agents and to chemotherapeutic agents used for colon cancer treatment (5-FU and OXA). Only the Plk1 inhibitor BI 2536 resulted in a >50% reduction of CCIC viability after 48 hours in two CCIC lines tested (Fig. 2C; Supporting Information Fig. S3B; compounds' names are shown in greater detail in Supporting Information Table 3). A dose-response assessment of BI 2536 efficacy revealed that CCIC death was induced already at a 25 nM concentration (Supporting Information Fig. S3C). However, we chose a working concentration of 100 nM, as this dose was previously shown to maximally and specifically inhibit Plk1 [15]. To investigate the in vitro sensitivity to Plk1 inhibitors of differently proliferating CCIC subsets separated according to PKH staining, we evaluated the colony-forming capacity of $PKH_{LOW/NEG}$, PKH_{MED}, and PKH_{HIGH} fractions in the presence of BI 2536. None of the three CCIC subsets was able to generate colonies in semisolid culture in the presence of BI 2536 (Fig. 2D), prompting us to use bulk CCIC cultures for subsequent experiments. The effect of BI 2536 was then tested on seven patient-derived CCIC lines, where it was able to inhibit colony formation in 6/7 cases (Fig. 2E). Importantly, BI 2536 was more effective than chemotherapeutic agents in reducing CCIC viability in six of seven CCIC lines tested (Fig. 2F). Finally, we compared the effect of BI 2536 on stem and differentiated colon cancer cells. As expected, CCIC resulted more sensitive than their differentiated progeny to Plk1 inhibition (Fig. 2G), according to their higher proliferative activity.

Plk1 Depletion Recapitulates the Effects of BI 2536 on Colon CSCs

Although highly specific for Plk1, BI 2536 can affect the activity of other Plks kinases such as Plk2 and Plk3 [15]. To confirm that the effects observed on CCIC were due to Plk1 inhibition, we specifically knocked down Plk1 expression by treating two CCIC lines with targeted short hairpin RNA (shRNA) sequences. Plk1 protein expression was effectively decreased in RNA interference (RNAi)-treated cells, as shown by immunoblot analysis of the two CCIC lines (Fig. 3A). After 48 hours of RNAi, CCIC with decreased Plk1 expression were characterized by spheroid disaggregation and by the appearance of cells with aberrant mitotic spindles (Fig. 3B). The viability of CCIC treated with Plk1 RNAi, but not with control oligonucleotides, massively decreased 72 hours after transfection (Fig. 3C), indicating that Plk1 is essential for CCIC survival and that its downregulation initiates cell death.

Plk1 Inhibition Subverts Cell Cycle Kinetics in CCIC

To investigate the consequences of Plk1 inhibition in CCIC, we treated spheroids with BI 2536 for 24 hours and observed

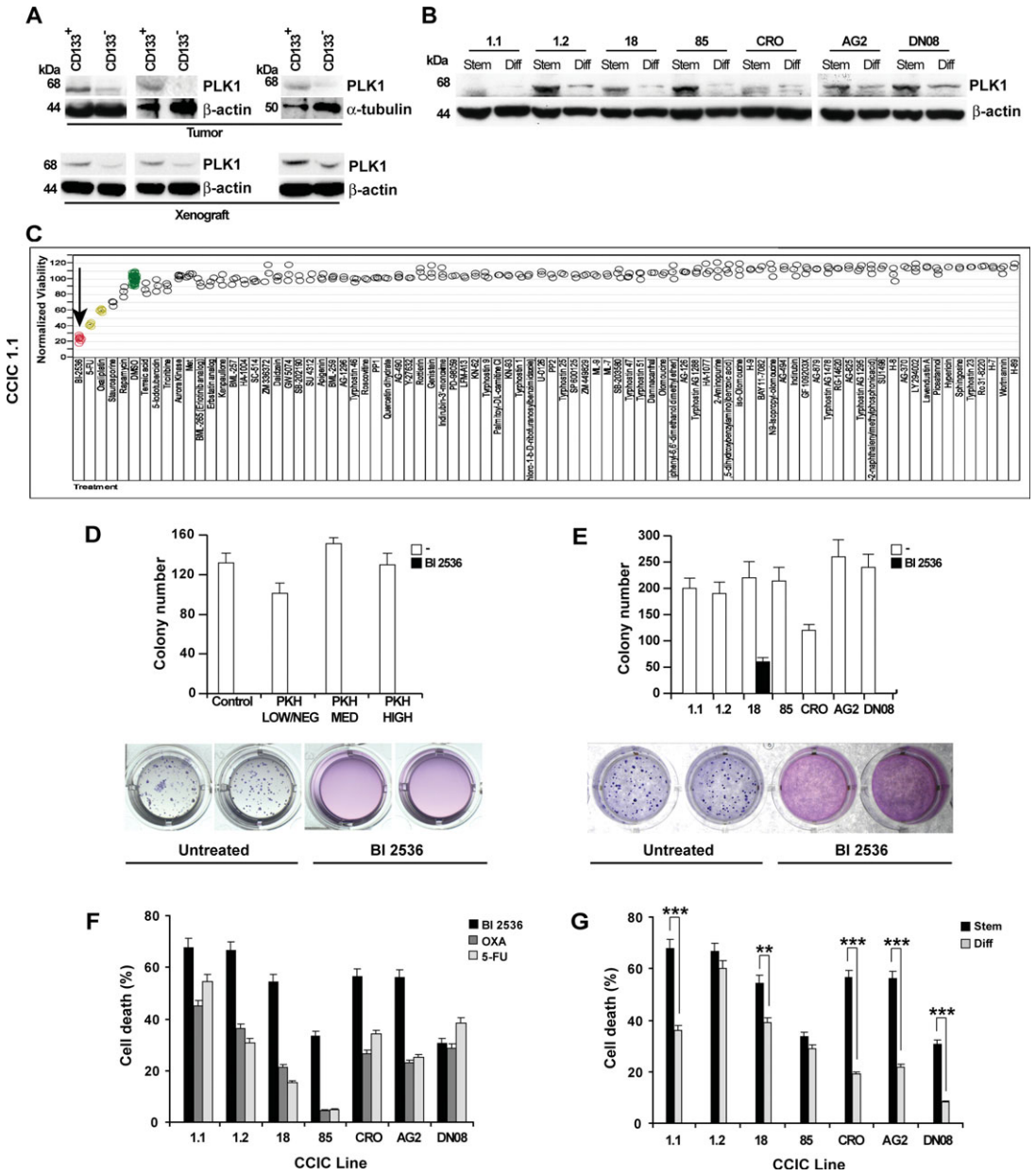

Figure 2. CCIC overexpress Plk1 and are specifically sensitive to Plk1 inhibitors. (**A**): Plk1 expression in $CD133^+$ and $CD133^-$ cells freshly isolated from three different colon adenocarcinoma samples (tumor) or from mouse xenografts derived from three different CCIC lines (xenograft). (**B**): Plk1 expression in CCIC (Stem) and in their differentiated counterparts (Diff). (**C**): Screening of kinase inhibitor library and chemotherapeutic agents on one CCIC line (CCIC 1.1). Cells were treated for 48 hours with the indicated compounds (shown in greater detail in Supporting Information Table 3), and cell viability was measured as described in Materials and Methods. The arrow indicates the BI 2536-treated sample. (**D**): Top: Colonies grown in soft-agar from $PKH_{LOW/NEG}$, PKH_{MED}, and PKH_{HIGH} fractions separated from one CCIC line (CCIC DN08), stained as in Figure 1 and plated in the presence (BI 2536) or in the absence (−) of 100 nM BI 2536. Bottom: Representative picture of the plates. (**E**): Top: Colonies generated in soft-agar by seven CCIC lines in the presence (BI 2536) or in the absence (−) of 100 nM BI 2536. Bottom: Representative picture of the plates. (**F**): Cell death induced by 100 nM BI 2536 (BI 2536) or chemotherapeutic agents OXA or 5-FU (10 μM each) in CCIC lines after 48 hours of treatment. (**G**): Cell death induced by 48 hours of treatment with BI 2536 in seven lines of CCIC (Stem) as compared with their differentiated progeny (Diff). ANOVA comparison of stem versus differentiated cells resulted in $p < .001$. Data shown in (D–G) are the mean ± SD of four independent experiments. **, $p < .01$; ***, $p < .001$. Abbreviations: CCIC, colon cancer-initiating cells; OXA, oxaliplatin; Plk1, Polo-like kinase1; 5-FU, 5-fluorouracil.

the appearance of mitotic nuclei in 20%–80% of cells (Fig. 4A, left) which, upon actin/tubulin staining, showed a disorganized cytoskeleton and mitotic spindles typical of the "Polo" phenotype (Fig. 4A, right) [16]. Propidium iodide staining of BI 2536-treated CCIC showed an accumulation of cells in the G2/M phase of the cell cycle (Fig. 4B). An evaluation of mitosis-associated proteins showed that BI 2536 treatment resulted in dephosphorylation/activation of Cdc2 and in cyclin B1 accumulation typical of prophase entry, as confirmed by massive histone H3 phosphorylation (Fig. 4C). At the same time, the Plk1 substrate Cdc25 was progressively dephosphorylated (Fig. 4C). In line with previous studies [15], we found cyclin B1 accumulation in the nucleus of BI 2536-treated cells, which was maximal at 8 hours (Fig. 4D). These

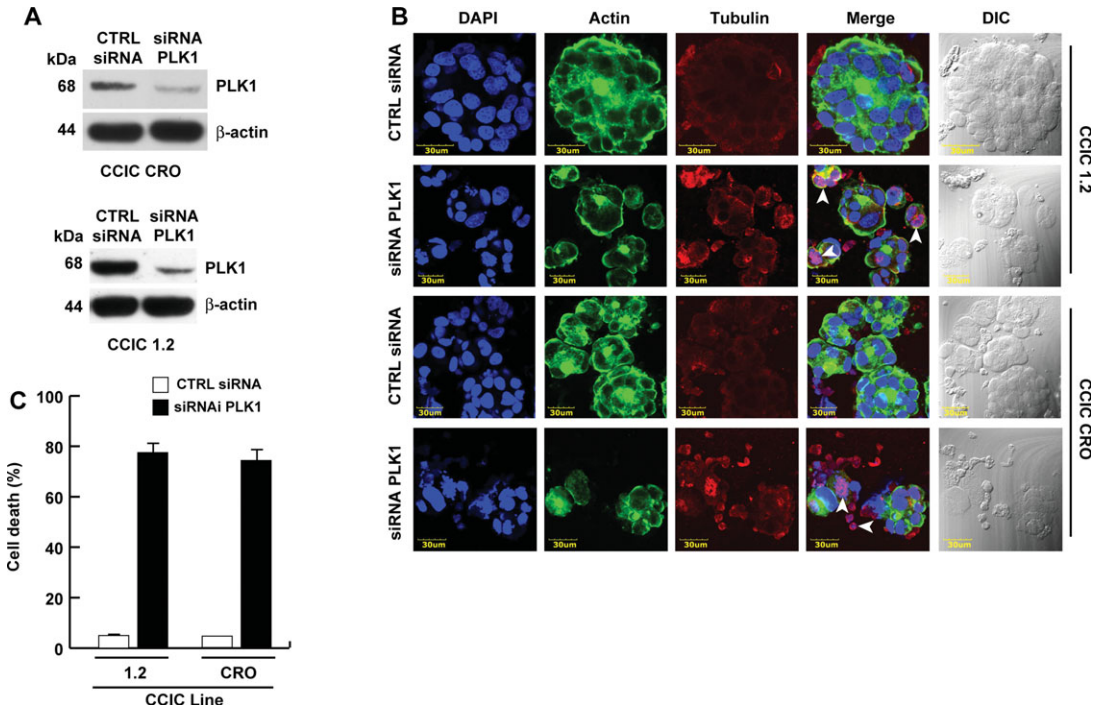

Figure 3. RNA interference against Plk1 results in CCIC death. (**A**): Plk1 expression detected 48 hours after transfection in two CCIC lines (CCIC 1.2 and CRO) transfected with control (CTRL siRNA) or anti-Plk1 (siRNA Plk1) RNA sequences. (**B**): Actin/tubulin staining performed 48 hours after transfection of two CCIC lines treated as in (A); white arrows indicate aberrant mitotic spindles. (**C**): Cell death detected 72 hours after transfection in two CCIC lines treated as in (A). Data shown are the mean ± SD of three independent experiments. Abbreviations: CCIC, colon cancer-initiating cells; DAPI, 4′,6-diamidino-2-phenylindole; DIC, differential interference contrast; Plk1, Polo-like kinase1; siRNA, short-interfering RNA.

observations confirm that Plk1 is dispensable for Cdc2 activation and cyclin B1 nuclear translocation at mitotic entry [17], whereas it is essential for Cdc25 phosphorylation in mitotic cells. Aurora A expression was also investigated upon treatment with BI 2536, as Aurora A plays an important role in CCIC and is tightly linked to Plk1 in the control of mitotic progression [18–20]. In untreated CCIC, intense Aurora A expression was detectable only in dividing cells, whereas the majority of BI 2536-treated cells expressed high Aurora A levels (Fig. 4E).

CCIC Respond to Plk1 Inhibitors with DNA damage, Mitochondrial Depolarization, and Mitotic Death

Acute Plk1 inhibition has been previously shown to induce apoptosis in cancer cell lines [15, 21–24]. Therefore, we analyzed the effect of BI 2536 in CCIC by assessing signs and mechanisms of cell death. First, we observed ATM phosphorylation/activation in CCIC after 4 hours of BI 2536 treatment and a progressive H2AX phosphorylation peaking at 48 hours, indicating the occurrence of a DNA damage response (Fig. 5A, 5B; Supporting Information Fig. S5A). Then, we evaluated typical hallmarks of apoptosis in treated cells. We found consistent mitochondrial depolarization both in intact spheroids (Fig. 5C) and in dissociated CCIC (Fig. 5D; Supporting Information Fig. S5B), cytochrome c release from mitochondria (Fig. 5E) and activation of caspases 3 and 9 (Fig. 5F). However, BI 2536-induced death of CCIC appeared to be mainly caspase-independent, as the pan-caspase inhibitor carbobenzoxy-valyl-alanyl-aspartyl-[O-methyl]-fluoromethylketone (zVAD-FMK) was unable to inhibit CCIC death, while it effectively blocked TNF-related apoptosis-inducing ligand (TRAIL)-induced apoptosis in Jurkat cells (Supporting Information Fig. S5C). In BI 2536-treated CCIC, the majority of cells acquired a giant size (Supporting Information Fig. S5D) and up to 10% of the cells became polyploid (Fig. 5G), indicating that CCIC undergo mitotic cell death in the presence of Plk1 inhibitors.

Plk1 Inhibition In Vivo Results in CCIC Death and Tumor Growth Arrest

CSC are characterized by the ability to reproduce the original human tumor in immunocompromised mice, thus representing a powerful tool to evaluate the effect of anticancer agents in vivo. We investigated the effect of Plk1 inhibition on CCIC-derived tumor xenografts obtained through subcutaneous injection of CCIC, which reproduced the histological structure of the parental colorectal tumor (Fig. 6A). For in vivo experiments we used BI 6727, a dihydropteridinone Plk1 inhibitor similar to BI 2536 with comparable activity toward CCIC in vitro (data not shown) and an improved pharmacokinetic profile in vivo [25]. Analysis of cell cycle and apoptosis markers performed on CCIC-derived xenografts upon a short-time treatment with BI 6727 revealed a widespread induction of histone H3 phosphorylation at 24 hours (Fig. 6B) indicating the occurrence of mitotic arrest in the majority of cells. Caspase 3 was massively activated in BI 6727-treated xenografts at 48 hours of treatment as shown by extensive staining for cleaved cytokeratin (Supporting Information Fig. S6A). Importantly, a double staining for CD133 and TUNEL on xenograft sections revealed that areas of cell death widely overlapped with stem cell areas identified by CD133 positivity in BI 6727-treated samples but not in chemotherapy-treated samples (Fig. 6C), indicating that BI 6727 specifically induces CCIC apoptosis in vivo. Similar results were obtained by double staining of xenografts sections with Lgr5 and TUNEL (Supporting Information Fig. S6B). A 21-day treatment with BI 6727 resulted in complete block of tumor growth, whereas standard chemotherapeutic agents (OXA plus 5-FU) were

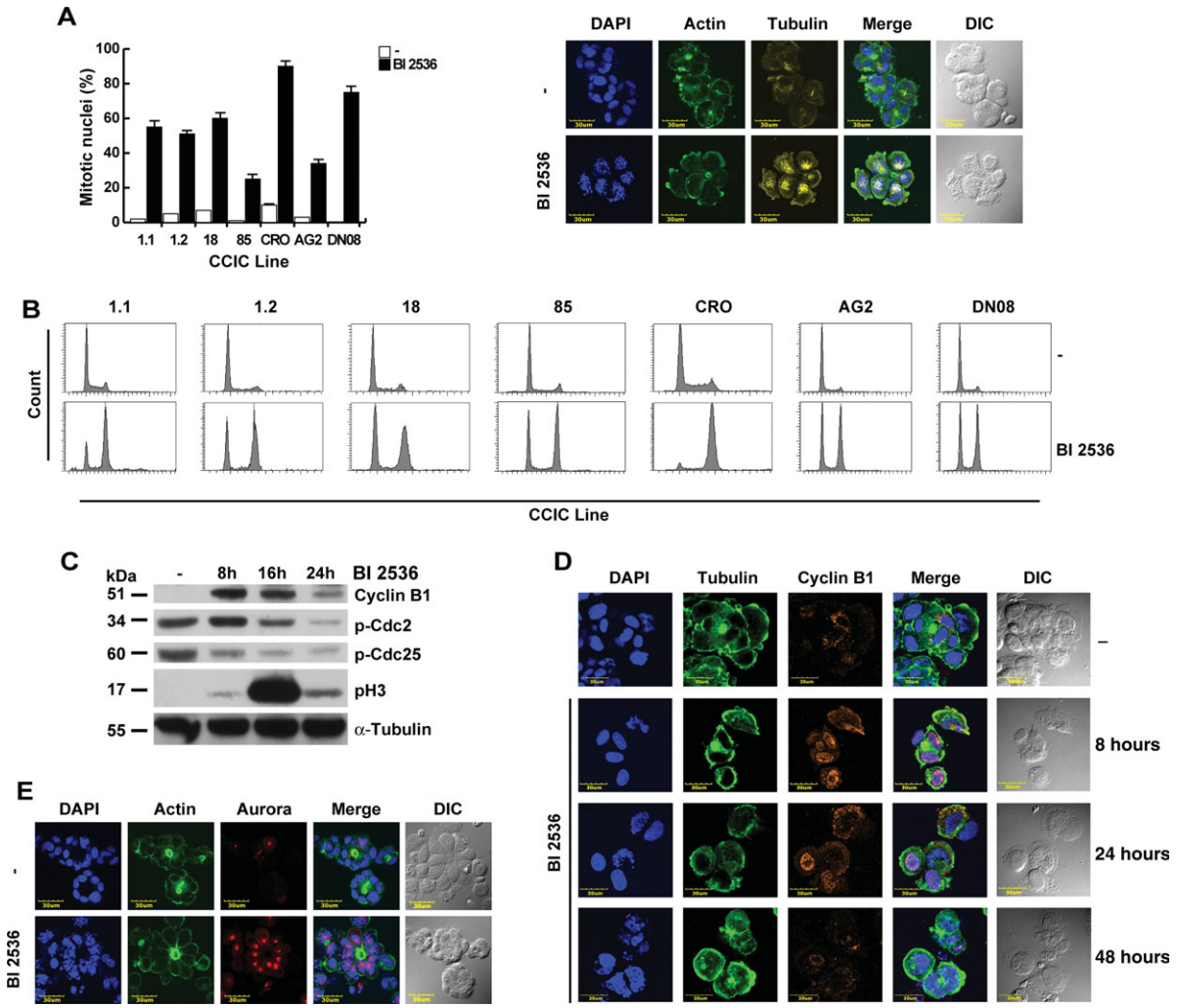

Figure 4. Plk1 inhibition by BI 2536 alters cell cycle kinetics in CCIC. (**A**): Percentage of mitotic nuclei in CCIC lines untreated (−) or treated for 24 hours with 100 nM BI 2536 (left) and actin/tubulin immunofluorescence staining of CCIC (AG2) treated for 24 hours with 100 nM BI 2536 (right). (**B**): Cell cycle analysis of CCIC treated for 24 hours with 100 nM BI 2536. Data shown are the mean ± SD of three independent experiments. (**C**): Western blot analysis of cyclin B1, p-Cdc2, p-Cdc25, and p-histone H3 (pH3) in the CCIC line AG2 untreated or treated for the indicated times with 100 nM BI 2536. (**D**): Immunofluorescence analysis of cyclin B1 localization in the CCIC line AG2, untreated or treated for the indicated times with 100 nM BI 2536. (**E**): Immunofluorescence analysis of Aurora A expression in the CCIC line AG2 untreated (−) or treated for 24 hours with 100 nM BI 2536 (BI 2536). Abbreviations: CCIC, colon cancer-initiating cells; Cdc, cell division cycle; DAPI, 4′,6-diamidino-2-phenylindole; DIC, differential interference contrast; Plk1, Polo-like kinase1.

only able to slow xenograft expansion (Fig. 6D). Assessment of tumor size and weight at the end of treatment confirmed that the growth of CCIC xenografts was strongly inhibited by BI 6727 and at a lesser extent by chemotherapeutic agents (Fig. 6E).

Quiescent CD133 Cells Escape BI 6727 Treatment but Retain Sensitivity to Subsequent Plk1 Inhibition

To investigate the long-term effects of BI 6727 on xenograft stem cell populations, we examined xenografts treated for 21 days with either chemotherapeutic agents or BI 6727. Azan-Mallory staining of xenograft sections revealed that BI 6727-treated tumors contained large fibrotic areas, whereas chemotherapy-treated tumors showed a dense cellular structure (Fig. 7A). A quantitative evaluation of $CD133^+$ cells present in tumor xenografts revealed that the percentage of $CD133^+$ cells was increased both in chemotherapy-treated samples and in BI 6727-treated samples as compared with vehicle-treated controls (Fig. 7B). However, taking into account xenograft volume at the end of the treatment, the absolute CCIC content at the end of the treatment proved to be significantly lower in BI 6727-treated samples as compared to both controls and chemotherapy-treated samples (Fig. 7C). Moreover, a double staining for CD133 and Ki67 on xenograft sections revealed that, in chemotherapy-treated tumors, $CD133^+$ cells were actively proliferating. Conversely, in BI 6727-treated tumors, residual $CD133^+$ cells were completely quiescent (Fig. 7D). These observations indicate that treatment with Plk1 inhibitors, although does not completely eradicate the $CD133^+$ population, eliminates all the proliferating tumorigenic cells. To understand whether CCIC that survived BI 6727 treatment developed resistance to Plk1 inhibition, we isolated $EpCAM^+/CD133^+$ cells from vehicle-treated and BI 6727-treated xenografts, kept them in culture for 4 weeks, and then treated them with BI 6727 in comparison with the parental CCIC line. Sensitivity to BI 6727 was virtually identical in the three populations (Fig. 7E), indicating that $CD133^+$ cells that survive treatment with Plk1 inhibitors in vivo do not

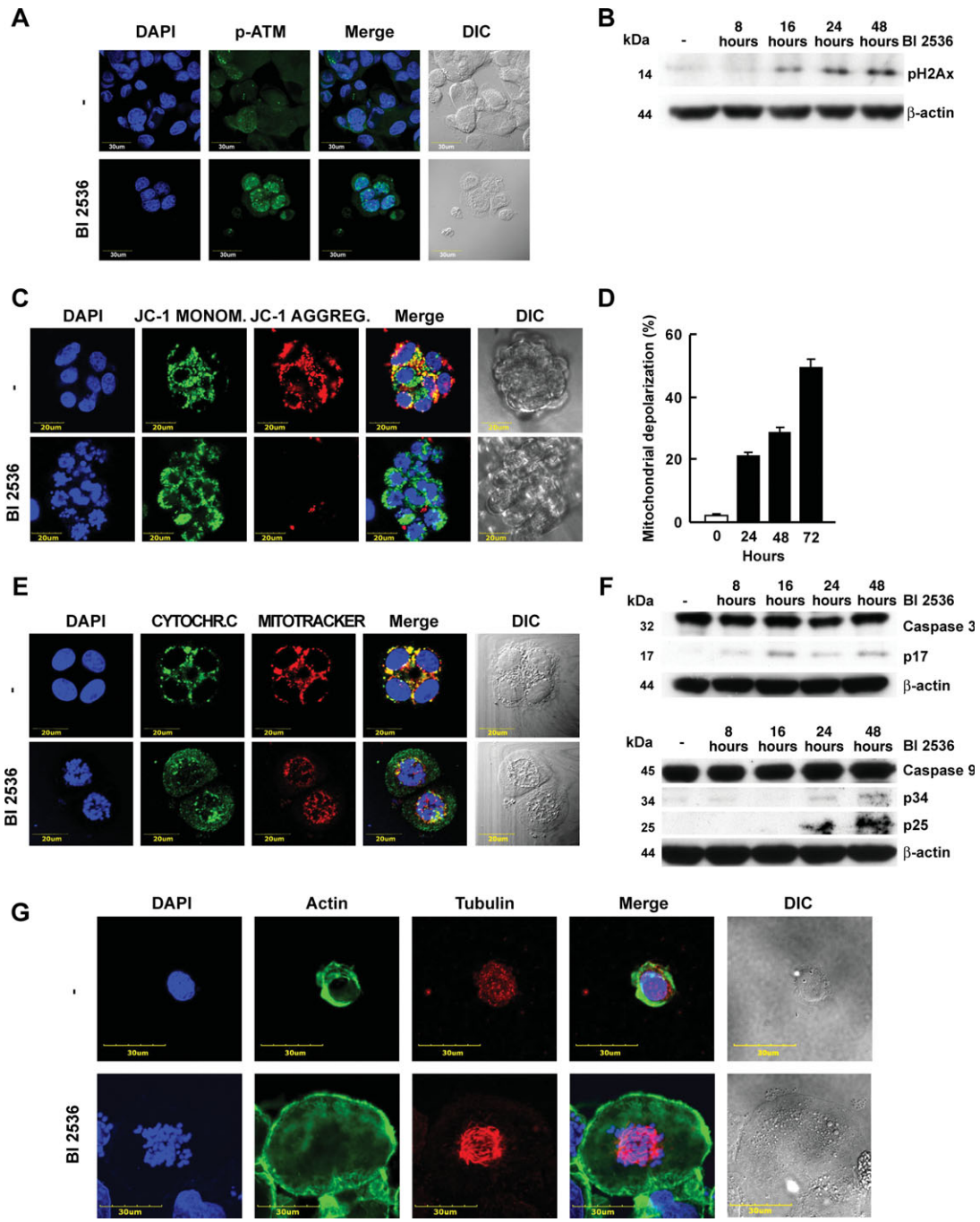

Figure 5. BI 2536 induces DNA damage and mitotic death of CCIC (line AG2). (**A**): ATM phosphorylation in CCIC, untreated (−) or treated for 4 hours with100 nM BI 2536. (**B**): Histone H2AX phosphorylation in CCIC untreated (−) or treated for 24 hours with 100 nM BI 2536. (**C**): Mitochondrial depolarization in live intact spheroids (JC-1 staining) treated for the indicated times with 100 nM BI 2536. ×60 magnification, ×2 zoom. (**D**): Mitochondrial depolarization in dissociated CCIC (TMRM staining) treated for the indicated times with 100 nM BI 2536. Data shown are the mean ± SD of three datasets obtained in independent experiments. (**E**): Cytochrome c release from mitochondria in CCIC untreated (−) or treated for 24 hours with 100 nM BI 2536 (BI 2536); ×60 magnification, ×2 zoom. (**F**): Activation of caspases 3 and 9 in CCIC treated for the indicated times with 100 nM BI 2536. (**G**): Actin/tubulin staining in untreated CCIC (−) compared with a giant polyploid CCIC obtained by treatment for 72 hours with 100 nM BI 2536 (×60 magnification, ×3 zoom). Abbreviations: ATM, ataxia-telangiectasia mutated; CCIC, colon cancer-initiating cells; DAPI, 4′,6-diamidino-2-phenylindole; DIC, differential interference contrast; Plk1, Polo-like kinase1; JC-1, 5,5′,6,6′-tetrachloro-1,1′,3,3′-tetraethylbenzimidazolyl carbocyanine iodide; TMRM, tetramethylrhodamine methyl ester.

acquire resistance to Plk1 inhibitors. Altogether these observations indicate that, in vivo, CCIC respond to chemotherapeutic agents with increased proliferation, whereas in the presence of Plk1 inhibitors CCIC are found in a quiescent state resulting in inhibition of tumor growth.

Discussion

Stem cells of normal adult tissues are predominantly found in a quiescent state, from which they egress to replenish the

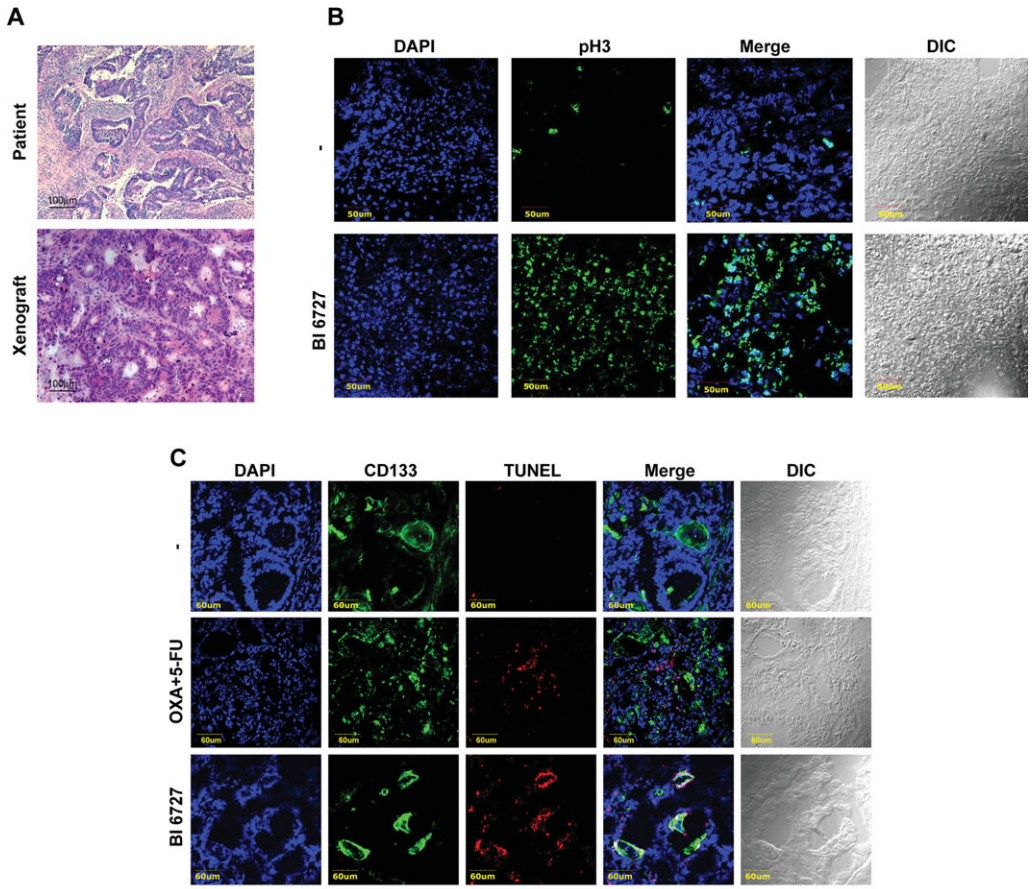

	Vehicle vs OXA+5-FU		Vehicle vs BI 6727		OXA+5-FU vs BI 6727	
Time (days)	P value	Summary	P value	Summary	P value	Summary
0	$p > .05$	ns	$p > .05$	ns	$p > .05$	ns
3	$p > .05$	ns	$p > .05$	ns	$p > .05$	ns
7	$p > .05$	ns	$p < .05$	*	$p > .05$	ns
10	$p > .05$	ns	$p < .01$	**	$p > .05$	ns
14	$p < .001$	***	$p < .001$	***	$p < .05$	*
17	$p < .001$	***	$p < .001$	***	$p < .01$	**
21	$p < .001$	***	$p < .001$	***	$p < .001$	***

Figure 6. Plk1 inhibitors target CCIC in vivo and block the growth of CCIC-derived xenografts. (**A**): Hematoxylin/Eosin staining of a CCIC-derived xenograft section (lower panel, cryosection) and of the parental patient tumor (upper panel, paraffin-embedded), ×10 magnification. (**B**): Phospho-histone H3 (pH3) staining of xenograft sections obtained from mice treated for 24 hours with vehicle (−) or with BI 6727 (BI 6727), ×60 magnification. (**C**): Immunofluorescence staining (×40 magnification) for CD133 and TUNEL of xenograft sections derived from mice treated for 48 hours with vehicle (−) or with BI 6727 (BI 6727). (**D**): Tumor volume of xenografts treated with vehicle only (vehicle), with chemotherapeutic agents (OXA+5-FU) and with BI 6727 (BI 6727) as described in Materials and Methods section. Statistical analysis is shown in the table beneath, where ns stands for "nonsignificant". Two-way ANOVA resulted in $p < .001$. The results shown are representative of four independent experiments. (**E**): Tumor weight at the end of treatment and representative picture. Data shown are the mean ± SD of six samples per group relative to the experiment shown in (D). *, $p < .05$; ***, $p < .001$. All the experiments in this figure were performed with the CCIC line AG2 and replicated on the CCIC line DN08 with similar results. Abbreviations: CCIC, colon cancer-initiating cells; DAPI, 4′,6-diamidino-2-phenylindole; DIC, differential interference contrast; OXA, oxaliplatin; Plk1, Polo-like kinase1; TUNEL, terminal deoxynucleotidyl transferase dUTP nick end labeling; 5-FU, 5-fluorouracil.

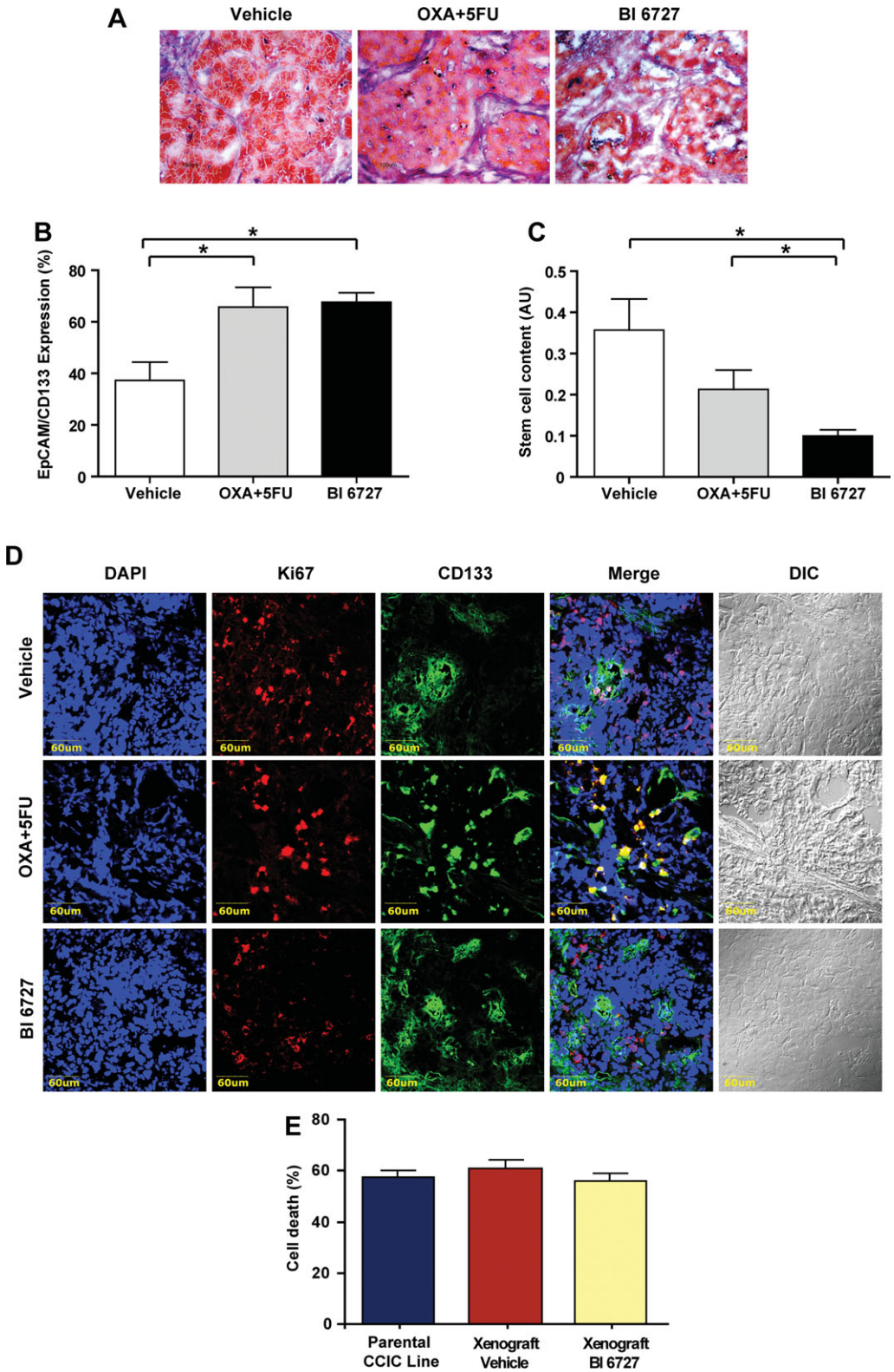

Figure 7. BI 6727-treated xenografts contain quiescent $CD133^+$ cells that retain sensitivity to Plk1 inhibitors. (**A**): Azan-Mallory staining of xenograft sections derived from vehicle-treated (vehicle), chemotherapy-treated (OXA+5-FU), and BI 6727-treated mice after 3 weeks of treatment. ×10 magnification. (**B**): Percentage of $CD133^+/EpCAM^+$ cells present in xenografts after 3 weeks of treatment with vehicle only (vehicle), chemotherapy (OXA+5-FU), or BI 6727. Data shown are the mean ± SD of five samples per group. (**C**): Total stem cell content in tumor xenografts relative to the experiment shown in Figure 6B. Values were calculated as tumor weight × percentage of $Epcam^+CD133^+$ cells/100. (**D**): Immunofluorescence staining (×40 magnification) of Ki67 and CD133 in xenograft sections obtained after 3 weeks of treatment with vehicle only (vehicle), chemotherapy (OXA+5-FU), or BI 6727. (**E**): Cell death induced by treatment in vitro with 100 nM BI 6727 for 48 hours of the parental CCIC line and of $EpCAM^+/CD133^+$ cells extracted from vehicle-treated (xenograft vehicle) or BI 6727-treated (xenograft BI 6727) xenografts after 3 weeks of in vivo treatment. Data shown are the mean ± SD of three samples per group. All the experiments in this figure were performed with the CCIC line AG2. Abbreviations: A.U.: arbitrary units; CCIC, colon cancer-initiating cells; DAPI, 4′,6-diamidino-2-phenylindole; DIC, differential interference contrast; EpCAM, epithelial cell adhesion molecule; OXA, oxaliplatin; Plk1, Polo-like kinase1; 5-FU, 5-fluorouracil.

pool of more differentiated cells. A similar hierarchy of proliferating cells is found in hematologic malignancies, where a population of quiescent stem cells retains the ability to transfer the disease in experimental animals, likely being responsible for drug resistance and relapse in leukemia patients. Differently from other stem cell types, normal colon stem cells have been found to be actively proliferating, both in mice and in humans [26, 27]. Proliferation of CSCs from solid tumors has been mainly investigated in breast cancer, where tumorigenic cells have been demonstrated to possess a replicative activity higher than their normal counterparts [7]. This feature, together with their predilection toward symmetric division, may be responsible for continuous expansion of the breast CSC population. Characterizing the proliferation state of CSCs has strong therapeutic implications, as identifying altered cell division mechanisms present in tumorigenic cells may indicate effective routes to eradicate this population. We found that CCIC comprise both rapidly and slowly proliferating cells. Consistently with a sustained proliferative activity in vivo, CCIC freshly isolated from colon cancer specimens express high levels of Plk1, a kinase essential for multiple steps of cell division. Although not specifically considered as part of the classic stem cell equipment, increased Plk1 expression was previously identified as part of a gene signature concomitantly altered in both normal stem cells and metastatic prostate cancer cells [28], suggesting the existence of a link between stemness and deregulated expression of Plk1. More generally, high Plk1 activity is considered as a tumor-promoting force, as it has been demonstrated to stimulate mitosis, override DNA damage checkpoints, support cell invasion, and facilitate the insurgence of aneuploidy [10].

Plk1 inhibitors have been recently demonstrated to be particularly cytotoxic for neuroblastoma tumor-initiating cells and for breast cancer-initiating cells, suggesting that they may represent an interesting therapeutic option in multiple tumor types [29, 30]. Our results demonstrate that, in colon tumors, the use of Plk1 inhibitors resulted in CCIC death both in vitro and in vivo, showing an increased efficacy over chemotherapeutic agents. Due to their enhanced antitumor effect as compared with conventional chemotherapy, Plk1 inhibitors may prove particularly useful in the preoperative setting, when a rapid reduction of tumor volume is required in order to perform radical surgery and/or preserving organ function. For instance, Plk1 inhibitors may be indicated for the preoperative treatment of colorectal cancer patients with unresectable liver metastatic disease. In this case, Plk1 inhibitors (which are not associated to significant hepatobiliary toxicity) would have a clear advantage over chemotherapeutic agents, which cause considerable liver damage further increasing liver injury due to hepatic metastases and surgical resection. To a similar extent, BI 6727 could be exploited in the neoadjuvant setting for treating rectal cancer patients; in this setting, there is an urgent need for identifying therapeutic options safer than standard chemoradiation protocols as well as to increase the rate of sphincter-preserving surgery when tumors arise from the distal rectum.

Specific analysis of CCIC proliferation state in xenografts treated for 3 weeks with chemotherapy or Plk1 inhibitors showed that chemotherapy-treated tumors, although smaller than control tumors, contained actively proliferating $CD133^+$ cells. Conversely, tumors treated with Plk1 inhibitors had a smaller size and contained only quiescent $CD133^+$ cells. These observations indicate that Plk1 inhibitors block tumor growth by eliminating all the proliferating tumorigenic cells. This situation reminds the effect of imatinib in chronic myeloid leukemia (CML), where the breakpoint cluster region-Abelson (BCR-ABL) inhibitor selectively eliminates proliferating leukemia cells [31, 32]. The inability of imatinib to eliminate quiescent stem cells, together with the propensity of neoplastic cells to acquire BCR-ABL kinase domain mutations results, in most cases, in persistence of the malignant CML clone. Differently, quiescent CCIC that survive treatment with Plk1 inhibitors in vivo do not acquire resistance to these drugs suggests that, in line of principle, they may be targeted by sequential rounds of BI 6727 treatment or by alternate rounds of chemotherapy/Plk1 inhibitors.

Conclusion

Our results indicate for the first time that colon cancer tumorigenic cells actively proliferate in vivo and are characterized by an elevated expression of Plk1, which constitutes a relevant therapeutic target. Future studies will be crucial to elucidate the mechanisms that control CSC quiescence and proliferation, as influencing this balance may render tumorigenic cells susceptible to targeted therapeutic strategies.

Acknowledgments

We are grateful to Stefano Guida for excellent technical assistance, Giuseppe Loreto for graphics, Marcello Maugeri for helpful discussion, Paola Simeone for animal care, Alessandra Boe for flow cytometry analysis, and Patrizio Rota for taking the picture in Figures 2D–2E. This work was financially supported by the Italian Association for Cancer Research (AIRC) and by the European Community's seventh Framework Programme grant agreement no. 202230. G.F. is supported by an Italy-USA ISS fellowship. BI 6727 was provided by Boehringer-Ingelheim (Austria, GmbH). His-Flag-TRAIL was kindly provided by T.L. Haas.

Disclosure of Potential Conflicts of Interest

The authors indicate no potential conflicts of interest.

References

1 Cunningham D, Atkin W, Lenz HJ et al. Colorectal cancer. Lancet 2010;375:1030–1047.

2 Bao S, Wu Q, McLendon RE et al. Glioma stem cells promote radioresistance by preferential activation of the DNA damage response. Nature 2006;444:756–760.

3 Eramo A, Ricci-Vitiani L, Zeuner A et al. Chemotherapy resistance of glioblastoma stem cells. Cell Death Differ 2006;13:1238–1241.

4 Diehn M, Cho RW, Lobo NA et al. Association of reactive oxygen species levels and radioresistance in cancer stem cells. Nature 2009; 458:780–783.

5 Vaiopoulos AG, Kostakis ID, Koutsilieris M et al. Colorectal cancer stem cells. Stem Cells 2012;30:363–371.

6 Maugeri-Sacca M, Vigneri P, De Maria R. Cancer stem cells and chemosensitivity. Clin Cancer Res 2011;17:4942–4947.

7 Cicalese A, Bonizzi G, Pasi CE et al. The tumor suppressor p53 regulates polarity of self-renewing divisions in mammary stem cells. Cell 2009;138:1083–1095.

8 Barker N, van Es JH, Kuipers J et al. Identification of stem cells in small intestine and colon by marker gene Lgr5. Nature 2007;449: 1003–1007.

9 Fenton B, Glover DM. A conserved mitotic kinase active at late anaphase–telophase in syncytial *Drosophila* embryos. Nature 1993;363: 637–640.

10 Strebhardt K. Multifaceted polo-like kinases: Drug targets and antitargets for cancer therapy. Nat Rev Drug Discov 2010;9:643–660.
11 Stadler WM, Vaughn DJ, Sonpavde G et al. Clinical outcome of single agent volasertib (BI 6727) as second-line treatment of patients (pts) with advanced or metastatic urothelial cancer (UC). In: ASCO ASoCo, ed. Paper presented at ASCO Annual Meeting, Chicago; 2011.
12 Ricci-Vitiani L, Lombardi DG, Pilozzi E et al. Identification and expansion of human colon-cancer-initiating cells. Nature 2007;445: 111–115.
13 O'Brien CA, Pollett A, Gallinger S et al. A human colon cancer cell capable of initiating tumour growth in immunodeficient mice. Nature 2007;445:106–110.
14 Huang EH, Hynes MJ, Zhang T et al. Aldehyde dehydrogenase 1 is a marker for normal and malignant human colonic stem cells (SC) and tracks SC overpopulation during colon tumorigenesis. Cancer Res 2009;69:3382–3389.
15 Lenart P, Petronczki M, Steegmaier M et al. The small-molecule inhibitor BI 2536 reveals novel insights into mitotic roles of polo-like kinase 1. Curr Biol 2007;17:304–315.
16 Steegmaier M, Hoffmann M, Baum A et al. BI 2536, a potent and selective inhibitor of polo-like kinase 1, inhibits tumor growth in vivo. Curr Biol 2007;17:316–322.
17 Gavet O, Pines J. Activation of cyclin B1-Cdk1 synchronizes events in the nucleus and the cytoplasm at mitosis. J Cell Biol 2010;189:247–259.
18 Macurek L, Lindqvist A, Lim D et al. Polo-like kinase-1 is activated by aurora A to promote checkpoint recovery. Nature 2008;455:119–123.
19 Seki A, Coppinger JA, Jang CY et al. Bora and the kinase Aurora a cooperatively activate the kinase Plk1 and control mitotic entry. Science 2008;320:1655–1658.
20 Cammareri P, Scopelliti A, Todaro M et al. Aurora-a is essential for the tumorigenic capacity and chemoresistance of colorectal cancer stem cells. Cancer Res 2010;70:4655–4665.
21 Lane HA, Nigg EA. Antibody microinjection reveals an essential role for human polo-like kinase 1 (Plk1) in the functional maturation of mitotic centrosomes. J Cell Biol 1996;135:1701–1713.
22 Cogswell JP, Brown CE, Bisi JE et al. Dominant-negative polo-like kinase 1 induces mitotic catastrophe independent of cdc25C function. Cell Growth Differ 2000;11:615–623.
23 Liu X, Erikson RL. Polo-like kinase (Plk)1 depletion induces apoptosis in cancer cells. Proc Natl Acad Sci USA 2003;100:5789–5794.
24 Spankuch-Schmitt B, Bereiter-Hahn J, Kaufmann M et al. Effect of RNA silencing of polo-like kinase-1 (PLK1) on apoptosis and spindle formation in human cancer cells. J Natl Cancer Inst 2002;94: 1863–1877.
25 Rudolph D, Steegmaier M, Hoffmann M et al. BI 6727, a Polo-like kinase inhibitor with improved pharmacokinetic profile and broad antitumor activity. Clin Cancer Res 2009;15:3094–3102.
26 Barker N, van de Wetering M, Clevers H. The intestinal stem cell. Genes Dev 2008;22:1856–1864.
27 Jung P, Sato T, Merlos-Suarez A et al. Isolation and in vitro expansion of human colonic stem cells. Nat Med 2011;17:1225–1227.
28 Glinsky GV, Berezovska O, Glinskii AB. Microarray analysis identifies a death-from-cancer signature predicting therapy failure in patients with multiple types of cancer. J Clin Invest 2005;115:1503–1521.
29 Grinshtein N, Datti A, Fujitani M et al. Small molecule kinase inhibitor screen identifies polo-like kinase 1 as a target for neuroblastoma tumor-initiating cells. Cancer Res 2011;71:1385–1395.
30 Hu K, Law JH, Fotovati A et al. Small interfering RNA library screen identified polo-like kinase-1 (PLK1) as a potential therapeutic target for breast cancer that uniquely eliminates tumor-initiating cells. Breast Cancer Res 2012;14:R22.
31 Graham SM, Jorgensen HG, Allan E et al. Primitive, quiescent, Philadelphia-positive stem cells from patients with chronic myeloid leukemia are insensitive to STI571 in vitro. Blood 2002;99:319–325.
32 Roeder I, Horn M, Glauche I et al. Dynamic modeling of imatinib-treated chronic myeloid leukemia: Functional insights and clinical implications. Nat Med 2006;12:1181–1184.


See www.StemCells.com for supporting information available online.